Connectome-based Modeling of Mnemonic Discrimination in Younger and Older Adults

Christopher N. Wahlheim[1,✉], Alexander P. Christensen[2], Zachariah M. Reagh[3], and Brittany S. Cassidy[1]

[1]Department of Psychology, University of North Carolina at Greensboro

[2]Department of Neurology, University of Pennsylvania

[3]Department of Psychological & Brain Sciences, Washington University in St. Louis

The ability to distinguish existing memories from similar perceptual experiences is a core feature of episodic memory. This ability is often examined using the Mnemonic Similarity Task in which people discriminate memories of studied objects from perceptually similar lures. Studies of the neural basis of such mnemonic discrimination have focused on hippocampal function and connectivity. However, default mode network (DMN) connectivity may also support such discrimination, given that the DMN includes the hippocampus, and its connectivity supports many aspects of episodic memory. Here, we used connectome-based modeling to identify associations between intrinsic DMN connectivity and mnemonic discrimination. We leveraged established discrimination deficits in older adults to test whether such age differences moderate network-wide relationships. Resting-state functional connectivity in the DMN predicted mnemonic discrimination ability outside the MRI scanner, especially among prefrontal and temporal regions and including several hippocampal regions. This predictive relationship was stronger for younger than older adults, with age differences primarily reflecting older adults' weaker temporal-prefrontal connectivity. These novel associations suggest that broader cortical networks including the hippocampus support mnemonic discrimination. They also suggest that disruptions within the DMN that emerge in healthy aging undermine the extent that the DMN supports this ability. These findings provide the first indication of how intrinsic functional properties of the DMN support mnemonic discrimination.

aging | default mode network | functional connectivity | hippocampus | lure discrimination

Correspondence: Department of Psychology, 296 Eberhart Building, P. O. Box 26170, University of North Carolina at Greensboro, Greensboro, NC, 27402-6170, USA; cnwahlhe@uncg.edu

Introduction

Encoding and retrieving everyday events allows people to relive past experiences and plan future behaviors. Because people experience countless overlapping events across a lifetime, they must be able to distinguish existing memories from perceptual inputs. For example, someone could leave the table during dinner and return to find a similar glass that is not theirs. One way they could avoid drinking from a similar glass is to discriminate the new glass from their memory for the original glass. The subsequent interference created by feature similarities such as these can be mitigated when one encodes the inputs (i.e., the glasses) as distinct representations. This encoding would allow one to avoid future confusion about the ownership of both glasses because each would be represented with unique contextual information. This pattern separation process is thought to be enabled by orthogonalization of overlapping inputs in the hippocampus (1–3). Evidence for pattern separation has been consistently inferred from studies showing that hippocampal function predicts mnemonic discrimination (for a review, see 4).

Substantial evidence for hippocampal involvement in mnemonic discrimination has been observed using modified recognition memory paradigms, such as the Mnemonic Similarity Task (MST; for a review, see 4). In the object version of the MST, people first study everyday objects (e.g., a glass). Then, on a subsequent memory test, people see some objects that are identical to studied objects (e.g., the same glass) and other objects that are perceptually similar but not identical to ones that were studied (e.g., an unstudied glass that is shorter than the studied glass). Mnemonic discrimination is operationalized as the ability to correctly reject these similar lures rather than classifying them as repeated items that were studied (i.e., false alarms). Research using functional magnetic resonance imaging (fMRI) has shown that mnemonic discrimination reliably evokes activity in hippocampal subfields (e.g., dentate gyrus and CA3) in paradigms that manipulate objects and scenes (5–8), spatial information (9, 10), and temporal intervals (9).

Although most studies have focused on the hippocampal computations that enable mnemonic discrimination, there is mounting evidence that neocortical regions also support this process (10–14). Recent fMRI studies have begun to characterize activation outside the hippocampus that supports mnemonic discrimination by examining whole-brain activity during the MST. For example, functional connectivity from the hippocampus to bilateral temporal regions as well as the cerebellum and frontal and temporal cortex has been shown during mnemonic discrimination (15). Other work has shown that activation in hippocampus as well as prefrontal and occipital cortex was associated with mnemonic discrimination (16), with the latter suggesting contributions of visual information that are not directly involved in discrimina-

tion (also see, 17). Further, widespread brain activity during mnemonic discrimination has been shown in default mode network (DMN; 18) regions, including the precuneus and angular gyrus (19), that was coupled with hippocampal activation during mnemonic discrimination. Finally, inactivation of anterior DMN regions (e.g., medial prefrontal cortex) in rodents has been shown to impair mnemonic discrimination (20). Together, these studies suggest that regional connectivity in the DMN may support mnemonic discrimination.

A potential role for DMN connectivity in mnemonic discrimination ability is also suggested by findings from intrinsic functional connectivity studies (i.e., connectivity during resting-state). Intrinsic DMN connectivity has been shown to support various episodic memory functions, such as autobiographical memory, prospection, and mental simulation (21, 22). During tasks, activity within specific DMN regions, such as precuneus, angular gyrus, temporopolar cortex, and medial prefrontal cortex, has been implicated in supporting episodic memory functions (23, 24). These DMN regions operate together with the hippocampus, a core structure involved in mnemonic discrimination, during episodic memory retrieval (25).

If intrinsic DMN connectivity also supports mnemonic discrimination, then this relationship should also be observed across a wide range of performance. One way to test this possibility is to examine whether this association occurs across groups that consistently differ in mnemonic discrimination, such as younger and older adults. Thus, testing people across age groups allows for examination of an important source of variability in mnemonic discrimination ability. Studies from the cognitive aging literature show poorer mnemonic discrimination abilities in groups of healthy older than younger adults (26). Hyperactivity in the hippocampus has been reliably linked to age-related mnemonic discrimination deficits (3, 13, 27, 28), and there is mounting evidence for age-related hypoactivity in MTL cortical regions (13, 27). Age-related dysfunction in the connectivity between anterior hippocampus and parahippocampal cortex is also associated with mnemonic discrimination deficits (29). Importantly, these findings in extrahippocampal areas suggest that network-level perturbations in aging may extend beyond the MTL into networks that support memory, such as the DMN.

An ideal method for examining the association between intrinsic functional connectivity of the DMN and mnemonic discrimination is Connectome-based Predictive Modeling (CPM; 30). CPM is a data-driven, leave-one-out cross-validation approach that builds a connectome associated with a specific behavior (e.g., mnemonic discrimination). A connectome is a set of functionally connected regions of interest (ROIs) used to predict the behavior of novel participants. CPM is favored over many related approaches, partly because it effectively predicts behavior using the connectivity between all ROIs without hypotheses about which connections will contribute (30). CPM has been used to identify whole-brain connectivity patterns at rest and during tasks that measure fluid intelligence (Finn et al., 2015), attentional control (31, 32), creative ability (33), and personality (34). It has also been used to characterize aspects of older adults' cognition (35). Together, this nascent literature suggests that the CPM approach is well-suited to explore the extent that intrinsic functional connectivity in DMN regions predicts mnemonic discrimination abilities in healthy younger and older adults.

The Present Study

Our overarching goal here was therefore to use CPM to characterize the relationships between intrinsic functional connectivity of the DMN and mnemonic discrimination in younger and older adults. After providing resting-state fMRI data, participants completed an object-based MST (26) and then a perceptual discrimination task (PDT), both outside of the scanner. This approach allowed us to isolate the relationships between neural activation and mnemonic processes in the following two primary aims.

Our first aim was to provide the first characterization of the association between intrinsic DMN connectivity and mnemonic discrimination using the CPM approach. Given the findings described above indicating that intrinsic DMN connectivity is associated with episodic memory, we expected that DMN connectivity would also positively predict mnemonic discrimination. Our rationale for this prediction is that mnemonic discrimination can be accomplished when similar lures trigger episodic retrievals of and comparisons with representations of studied objects. We also structured the CPM analyses to connect with studies examining hippocampal contributions to mnemonic discrimination (for a review, see 4). Specifically, we included in the CPM distinct regions for the hippocampal head, body, and tail to determine whether predictive inter-region connections differed along regions of the hippocampal longitudinal axis. We did not have any a priori hypotheses about these exploratory analyses.

Our second aim was to examine the extent that DMN connectivity predicts mnemonic discrimination in younger and older adults. Older adults consistently show impaired mnemonic discrimination (for a review, see 4) and weakened intrinsic DMN connectivity associated with episodic memory deficits (36, 37). Consequently, weaker intrinsic DMN connectivity in older than younger adults may undermine the extent that DMN connections predict older adults' mnemonic discrimination in the CPM. We therefore hypothesized that intrinsic DMN connectivity in the CPM would positively predict mnemonic discrimination more strongly for younger than older adults.

Method

The materials, anonymized data files, coded recall responses, and analysis scripts are available on the Open Science Framework (OSF): https://osf.io/f6vg8/. The study was approved by the University of North Carolina at Greensboro Institutional Review Board.

Participants. The participants were 36 younger and 36 older adults from the greater Greensboro, North Carolina community. They were right-handed and had no recent history

Table 1. Demographic Information and Cognitive Ability Scores for Younger and Older Adults

	Younger	Older	t	p	Cohen's d
Years of education	15.85 (2.50)	15.75 (2.29)	0.17	= .867	0.04
Vocabulary	29.03 (3.97)	33.64 (3.12)	5.01	< .001	1.29
Processing speed	78.26 (13.27)	63.36 (3.12)	4.51	< .001	1.15
Digit span (forward)	8.71 (2.14)	8.00 (2.09)	1.31	= .196	0.33
Digit span (backward)	7.38 (2.22)	6.82 (1.74)	1.09	= .280	0.28
MoCA	28.26 (1.42)	27.68 (1.39)	1.63	= .108	0.41

Note. Means and standard deviations (in parentheses) are displayed above. Vocabulary was quantified via the Shipley Vocabulary Test; Processing Speed was quantified via Digit Comparison Task; digit span scores were measured via tasks included in the Wechsler Memory Scales.

of neurological problems. The stopping rule was to collect usable data from at least 25 participants per age group. This sample size is comparable to research examining associations between functional connectivity and mnemonic discrimination in younger and older adults (29). We excluded one younger and one older adult who scored below 26 on the Montreal Cognitive Assessment (MoCA; 38). We also excluded one younger adult for excessive movement in the scanner, five older adults for responding on fewer than 70% of the MST trials, and two older adults for not following instructions. The final sample included 34 younger adults (18-32 years old, M_{age} = 22.21, SD = 3.65; 20 female) and 28 older adults (61-80 years old, M_{age} = 69.82, SD = 5.64; 20 female). Table 1 shows that younger and older adults had comparable education and working memory capacity, the latter measured by forward and backward digit span (39). Older adults had higher vocabulary scores (40) and slower processing speed (41) than younger adults.

Behavioral Tasks. Participants were tested individually in a quiet room. An experimenter explained the instructions before each task and then allowed participants to complete the task alone. Stimuli were presented electronically using E-Prime 3.0 software (42) on a PC laptop that included a 13.3 in (33.78 cm) display (1920 × 1080 resolution). The viewing distance was approximately 20 in (51 cm). Images of everyday objects (400 × 400 pixels) came from a publicly available database (https://github.com/celstark/MST) and included objects from the three sets that most taxed mnemonic discrimination (i.e., bins 1–3).

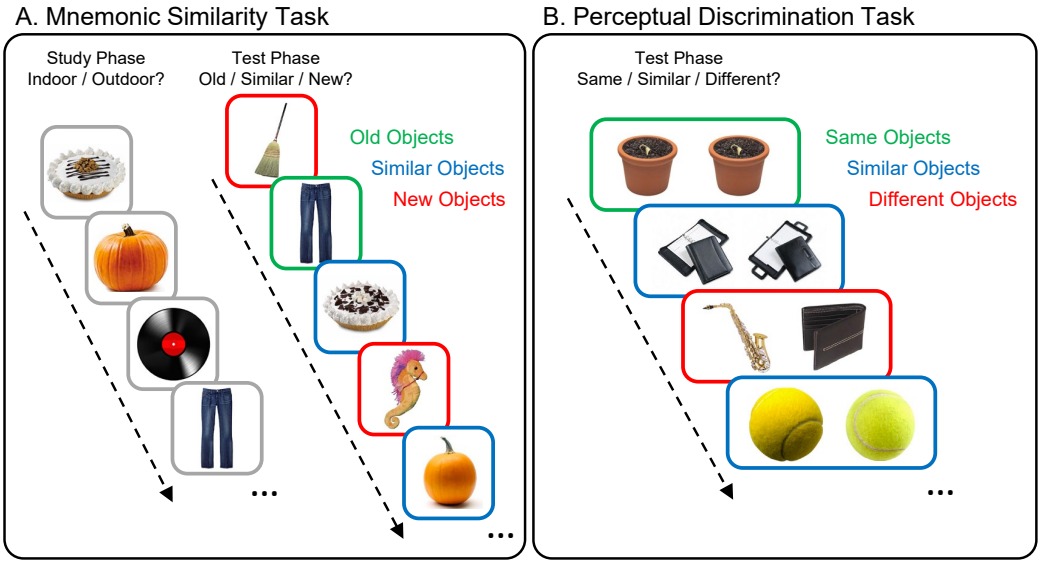

Fig. 1. Schematics of Behavioral Tasks. (A) In the Mnemonic Similarity Task, participants studied pictures of objects and took a recognition test in separate phases. The recognition test included old objects that were repeated from the study phase, similar objects that were alternative versions of other old objects from the study phase, and new objects that only appeared in the test phase. During study, participants indicated whether each object belonged indoors or outdoors. At test, participants indicated whether objects were old, similar, or new. (B) In the Perceptual Discrimination Task, two objects appeared side-by-side on each trial. Some pairs included two pictures of the exact same object, others included two similar versions of the same object, and another set included two different objects. Participants responded to each pair by indicating whether they included the same, similar, or different objects.

Mnemonic Similarity Task. Participants first completed a version of the object-based MST (Figure 1A) that included separate study and test phases. During study, pictures of everyday objects appeared in the center of the display against a white background for 2000 ms each. Participants pressed a key to indicate if the object belonged indoors (v) or outdoors (n). At test, participants viewed three object types for 2000 ms each. Objects were either exact repetitions of studied objects (old objects), similar lures that were same identity but different versions of studied objects (similar objects), or foils that were new (new objects). Participants pressed a key to classify objects as "old" (v), "similar" (b), or "new" (n). Objects appeared in random order in each phase. Each participant viewed 72 study objects and 108 test objects. The test included 36 old, 36 similar, and 36 new. Each 36-object set comprised 12 objects from each lure bin. The normative false alarm rates were equated across sets. For counterbalancing, object sets were rotated through conditions, creating three experimental formats.

Perceptual Discrimination Task. After the MST, participants completed the PDT (Figure 1B). The PDT was included to account for the role of age differences in perceptual ability in mnemonic discrimination performance (43). The PDT and MST included different objects to prevent MST experience from contaminating PDT performance. Normative false alarm rates for similar lure objects were equated across the tasks to control for stimulus effects. Participants were instructed to classify relationships within pairs. Two objects appeared together on each trial until participants responded. Participants pressed a key to classify pairs as comprising the "same" objects (v), "similar" objects (b), or "different" objects (n). Same pairs included identical objects (e.g., the same potted plant); Similar pairs included two versions of an object that could serve as a studied object and its similar lure in the MST (e.g., two similar day planners); and Different pairs included objects with different identities (e.g., a saxophone and a wallet). Pairs appeared in random order. There were 90 total pairs (36 same, 36 similar, and 18 different) including 18 unique object identities per condition (54 identities). For counterbalancing, object sets were rotated through within-subjects conditions, creating three experimental formats.

fMRI Data Acquisition and Preprocessing. Before completing the behavioral tasks, but after completing the neuropsychological measures, whole-brain imaging was performed on a Siemens 3.0T Tim Trio MRI Scanner using a 16-channel head coil at the Gateway MRI Center at the University of North Carolina at Greensboro. High-resolution anatomical images were acquired with a multi-planar rapidly acquired gradient echo (MP-RAGE) sequence (192 sagittal slices, 1 mm thickness, TR = 2300 ms, TE = 2.26 ms, 1.0 mm isotropic voxels). Resting-state functional data were collected after the anatomical scan. Resting-state data comprised 300 measurements collected over one 10-minute run. This scan duration produces reliable functional connectivity estimates within and across participants (44). Participants were instructed to remain still and awake with their eyes open. No stimuli appeared during this scan, and the display was black. Functional scans were collected using an echo-planar image sequence sensitive to blood-oxygen-level-dependent contrast (T2*; 32 slices with 4.0 mm thickness and no skip, TE = 30 ms, TR = 2000 ms, flip angle = 70, FOV = 220 mm, A/P phase encoding direction). Slices were collected in a descending order that covered the entire cortex and partial cerebellum. At the beginning of the resting-state scan, the scanner acquired and discarded two dummy scans.

Data were preprocessed using SPM12 (Wellcome Trust Centre for Neuroimaging, London, UK; www.fil.ion.ucl.ac.uk/spm). Images were: realigned to correct for motion, slice-time corrected, normalized to the MNI template, resampled to 3 mm isotropic voxels, and smoothed using an 8 mm FWHM isotropic Gaussian kernel. This smoothing precludes biases associated with spatial registration to a template across age groups (e.g., 45). The preprocessed resting-state data were submitted to the CONN functional connectivity toolbox (46) to test for motion artifacts and to create connectivity matrices for each participant.

Resting-state data were analyzed using custom artifact detection software (http://www.nitrc.org/projects/artifact_detect) to detect outlier time points for each participant. Following recommended conservative parameters for examining associations between DMN connectivity and age differences in behavior (47), volumes were excluded if the signal for that time point fell three standard deviations outside the mean global signal for the entire run or if the scan-to-scan head motion exceeded .5 mm in any direction. Volumes were excluded from further analyses using participant-regressors of no interest. Other nuisance regressors were the motion regressors obtained from the realignment step during preprocessing, white matter, cerebral spinal fluid (CSF), and other variables of no interest. Data were cleaned using the principal components analysis approach described in (46). This approach preserves valid positive functional connectivity estimates while controlling for the inflation of negative estimates and it regresses out physiological noise from areas of non-interest (e.g., white matter; see 48).

Stable correlations can be computed from resting-state functional data using around five minutes of cleaned data (49, 50). One younger adult was excluded for not meeting this threshold. The analyzed sample (34 younger and 28 older adults) showed patterns typical in aging and connectivity work (e.g., 47). There were more outliers scans for older adults (M = 34.71, SD = 29.15) than younger adults (M = 19.47, SD = 20.31), $t(60) = 2.42$, $p = 0.019$, $d = 0.61$. After removing these scans, younger adults retained an average of 9.36 minutes ($SD = 0.67$; 94% of the total 10 minutes) and older adults retained an average of 8.84 minutes ($SD = 0.97$; 88% of the total 10 minutes) of data. The residual time series was band-pass filtered in the 0.008–0.08 Hz range.

Functional connectivity matrices were calculated across the time series using Fisher's z coefficients between 200 cortical ROIs isolated using the Schaefer parcellation based on

the MNI template (51) and eight hippocampal regions (left and right medial and lateral head, left and right body, and left and right tail) extracted from the Melbourne Subcortex Atlas using the 2 mm group parcellation (52). Because there was

Table 2. MNI Coordinates of Tian and Schaefer Atlases

				MNI Coordinates			
Atlas	Hemisphere	ROI	Alphanumeric Code	X	Y	Z	NeuroSynth Locations
Tian	Left	Hippocampal Head	LH Head	-23	-14	-20	Hippocampus
Tian	Right	Hippocampal Head	RH Head	25	-14	-20	Hippocampus
Tian	Left	Hippocampal Body	LH Body	-28	-28	-10	Hippocampus
Tian	Right	Hippocampal Body	RH Body	30	-28	-10	Hippocampus
Tian	Left	Hippocampal Tail	LH Tail	-22	-38	-2	Hippocampus
Tian	Right	Hippocampal Tail	RH Tail	24	-38	-2	Hippocampus
Schaefer	Left	Ventral Prefrontal	LH PFCv 1	-35	20	-13	Insula
Schaefer	Left	Ventral Prefrontal	LH PFCv 2	-32	42	-13	Orbitofrontal
Schaefer	Left	Ventral Prefrontal	LH PFCv 3	-46	31	-7	Inferior Frontal Gyrus
Schaefer	Left	Ventral Prefrontal	LH PFCv 4	-52	22	8	Inferior Frontal Gyrus
Schaefer	Right	Ventral Prefrontal	RH PFCv 1	51	28	0	Insula
Schaefer	Left	Medial Prefrontal	LH PFCm 1	-6	36	-10	Ventromedial Prefrontal
Schaefer	Left	Medial Prefrontal	LH PFCm 2	-12	63	-6	Orbitofrontal
Schaefer	Left	Medial Prefrontal	LH PFCm 3	-6	44	7	Anterior Cingulate
Schaefer	Right	Medial Prefrontal	RH PFCm 1	8	42	4	Anterior Cingulate
Schaefer	Right	Medial Prefrontal	RH PFCm 2	6	29	15	Anterior Cingulate
Schaefer	Right	Medial Prefrontal	RH PFCm 3	8	58	18	Medial Prefrontal
Schaefer	Left	Dorsal Prefrontal	LH PFCd 1A	-24	25	49	—
Schaefer	Left	Dorsal Prefrontal	LH PFCd 1B	-8	59	21	Medial Prefrontal
Schaefer	Left	Dorsal Prefrontal	LH PFCd 2	-11	47	45	Medial Prefrontal
Schaefer	Left	Dorsal Prefrontal	LH PFCd 3	-3	33	43	Medial Prefrontal
Schaefer	Left	Dorsal Prefrontal	LH PFCd 4	-9	17	63	Pre-Supplementary
Schaefer	Right	Dorsal Prefrontal	RH PFCd 1A	29	30	42	—
Schaefer	Right	Dorsal Prefrontal	RH PFCd 1B	15	46	44	Medial Prefrontal
Schaefer	Left	Temporal	LH Temp 1	-47	8	-33	Anterior Temporal
Schaefer	Left	Temporal	LH Temp 2	-60	-19	-22	Lateral Temporal
Schaefer	Left	Temporal	LH Temp 3	-56	-6	-12	Superior Temporal
Schaefer	Left	Temporal	LH Temp 4	-58	-30	-4	Middle Temporal
Schaefer	Right	Anterior Temporal	RH AntTemp 1	47	13	-30	Anterior Temporal
Schaefer	Right	Temporal	RH Temp 1	63	-27	-6	Superior Temporal
Schaefer	Left	Parahippocampus	LH PHC 1	-26	-32	-18	Parahippocampus
Schaefer	Right	Parahippocampus	RH PHC 1	28	-36	-14	Parahippocampus
Schaefer	Left	Retrosplenial	LH Rsp 1	-11	-56	13	Retrosplenial
Schaefer	Right	Retrosplenial	RH Rsp 1	12	-55	15	Retrosplenial
Schaefer	Left	Posterior Cingulate	LH PCC 1	-5	-55	27	Posterior Cingulate
Schaefer	Left	Posterior Cingulate	LH PCC 2	-4	-31	36	Posterior Cingulate
Schaefer	Left	Posterior Cingulate	LH PCC 3	-6	-54	42	Precuneus
Schaefer	Right	Posterior Cingulate	RH PCC 1	7	-49	31	Posterior Cingulate
Schaefer	Left	Inferior Parietal	LH IPL 1A	-46	-66	38	Angular Gyrus
Schaefer	Left	Inferior Parietal	LH IPL 1B	-57	-54	28	Angular Gyrus
Schaefer	Left	Inferior Parietal	LH IPL 1C	-39	-80	31	Angular Gyrus
Schaefer	Right	Inferior Parietal	RH IPL 1A	54	-50	28	Angular Gyrus
Schaefer	Right	Inferior Parietal	RH IPL 1C	47	-69	27	Angular Gyrus

Note. The alphanumeric codes are the labels for the coordinates in the atlases that also appear in Figure 4. The ROIs appear in the same order as in Figure 4, starting from the top of the y-axis and the left of the x-axis. The NeuroSynth locations were extracted from the associations with meta-analysis maps.

no a priori reason to include medial and lateral hippocampal head ROIs, the medial and lateral hippocampus Fisher's z coefficients were averaged for left and right hemisphere. All z coefficient values were then transformed to Pearson's r correlation coefficients for ease of interpretation. Functional connectivity matrices were then constrained to the 37 ROIs labeled in the parcellation as being part of the DMN and the six hippocampal regions—bilateral head, body, and tail—for the CPM analyses described below (Table 2 contains MNI coordinates for each ROI). There was thus one 43 × 43 functional connectivity matrix per participant.

Results

The following results sections report findings from the behavioral tasks first to confirm the expected patterns of memory and perceptual discrimination performance. Following that, results from the CPM analyses are reported to establish a connectome that uniquely predicts mnemonic discrimination ability and that does not predict other distinct mnemonic and perceptual abilities (i.e., traditional recognition and perceptual discrimination).

Results from Behavioral Tasks.

Statistical Approach for Assessing Mnemonic and Perceptual Abilities. All analyses were conducted using R software (53). Linear regression models from base R included subjects as a random effect and experimental variables described below as fixed effects. Hypothesis tests were conducted using the `Anova` function from the *car* package (54) with Type III models to accommodate the different sample sizes for each age group. Pairwise comparisons were conducted using the `emmeans` function from the *emmeans* package (55). Exact model specifications are available in the analysis scripts on the OSF: https://osf.io/f6vg8/. The level for significance was set at $\alpha = .05$.

Mnemonic Similarity Task. Studies examining age differences in MST performance report response accuracy for each object type along with bias-corrected traditional recognition and mnemonic discrimination indices (26, 56). These studies consistently show that age-related memory deficits are selective for discrimination of similar lures from studied objects, with little if any deficits observed for traditional recognition. This selective deficit has been interpreted as showing that older adults experience pattern separation deficits. This analytic approach was followed here to verify that such differences were present in the current samples. Overall response patterns were characterized by computing probabilities for each object type between age groups (Table 3). Note that because test objects appeared briefly, participants did not respond on every trial. Therefore, probabilities of missing responses were also included in Table 3 and in the models. Bias-corrected mnemonic discrimination was estimated as the difference in "similar" responses for similar lure and new foil objects [p(similar | similar objects) – p(similar | new objects)]. This measure is referred to as the Lure Discrimination Index (LDI; see 4). Bias-corrected traditional recognition was estimated as the difference in "old" responses for old studied and new foil objects [p(old | old objects) – p(old | new objects)] to test for selective age-related deficits.

Impaired Mnemonic Discrimination in Older Adults. Mnemonic discrimination was first assessed by examining responses for similar objects (Table 3, left columns). A 2 (Age) × 4 (Response) model indicated no significant effect of Age, $F(1, 240) = 0.18$, $p = .67$, $\eta_p^2 < .01$, and a significant effect of Response, $F(3, 240) = 151.59$, $p < .001$, $\eta_p^2 = .79$. Participants made significantly fewer similar than old responses, $t(240) = 13.80$, $p < .001$, $d = 2.49$, which was not surprising because the paradigm included the most confusable lures. Participants also made significantly more similar than new and missing responses, smallest $t(240) = 11.46$, $p < .001$, $d = 2.07$, and no significant difference between the latter responses, $t(240) = 1.35$, $p = .53$, $d = 0.24$. There was also a significant Age × Response interaction, $F(3, 240) = 14.36$, $p < .001$, $\eta_p^2 = .15$, showing that younger adults made significantly more similar responses than older adults, $t(240) = 5.44$, $p < .001$, $d = 1.39$, and older adults made significantly more old responses than younger adults, $t(240) = 3.10$, $p = .04$, $d = 0.79$. This pattern suggested that mnemonic discrimination was better for younger than older adults. This interpretation was supported by the results of a model comparing LDI scores between age groups (Figure 2A) that showed significantly better bias-corrected mnemonic discrimination for younger than older adults, $t(60) = 3.27$, $p < .01$, $d = 0.84$.

No Age Differences in Traditional Recognition. Traditional recognition memory for studied objects was first assessed by examining responses for old objects (Table 3, middle

Table 3. Response Probabilities on the Mnemonic Similarity Task

	Object Type					
	Similar Objects		Old Objects		New Objects	
Response	Younger	Older	Younger	Older	Younger	Older
Similar	.38 [.34, .42]	.23 [.18, .27]	.08 [.06, .10]	.07 [.04, .09]	.12 [.08, .15]	.13 [.09, .16]
Old	.53 [.50, .57]	.62 [.59, .67]	.87 [.85, .89]	.86 [.84, .88]	.04 [.01, .07]	.03 [.01, .07]
New	.07 [.03, .10]	.08 [.04, .12]	.03 [.01, .05]	.04 [.02, .06]	.82 [.79, .86]	.75 [.75, .79]
Missing	.02 [.00, .06]	.07 [.03, .11]	.02 [.00, .04]	.03 [.01, .06]	.02 [.00, .05]	.09 [.05, .12]

Note. 95% confidence intervals are displayed in brackets.

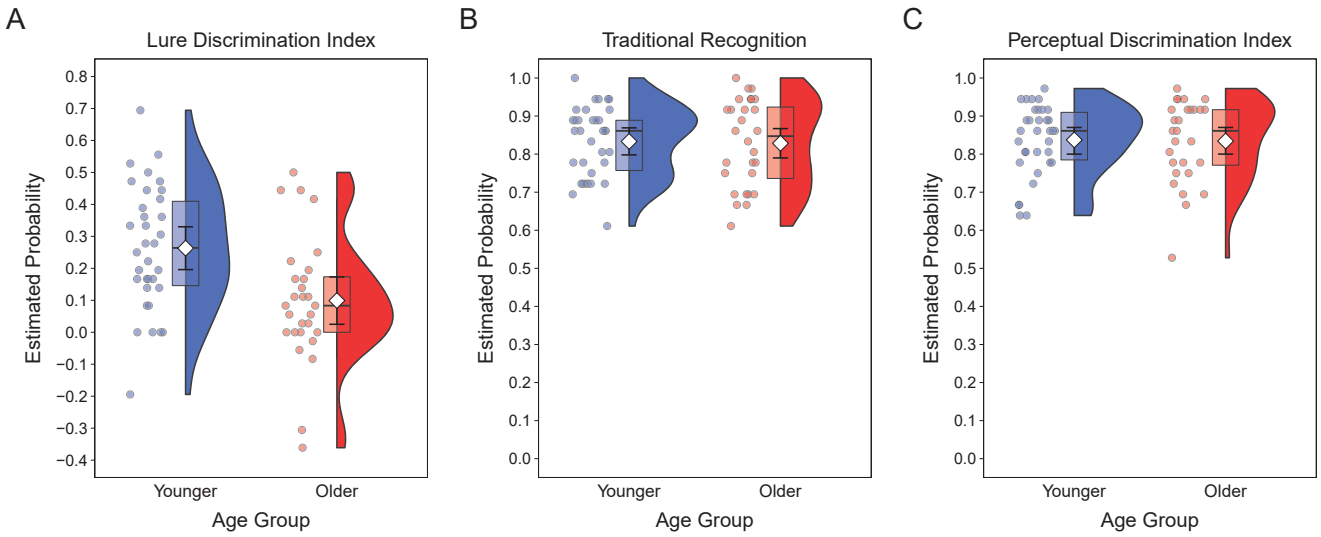

Fig. 2. Behavioral Task Performance. (A) Mnemonic discrimination, indicated by Lure Discrimination Index scores, was better for younger than older adults. (B) Recognition, indicated by Traditional Recognition scores, did not differ between age groups. (C) Perceptual discrimination, indicated by Perceptual Discrimination Index scores, did not differ between age groups. (All Panels) Colored points are individual participant probabilities, the widths of the half violin plots represent the proportion of data at each probability, box plots show interquartile ranges and medians, white diamonds are means, and errors bars are 95% confidence intervals.

columns). A 2 (Age) × 4 (Response) model indicated no significant effect of Age, $F(1, 240) = 0.14$, $p = .71$, $\eta_p^2 < .01$, a significant effect of Response, $F(3, 240) = 1133.91$, $p < .001$, $\eta_p^2 = .97$, and no Age × Response interaction, $F(3, 240) = 0.79$, $p = .50$, $\eta_p^2 < .01$. Participants made significantly more old than similar responses, $t(240) = 68.84$, $p < .001$, $d = 12.42$, and significantly more similar than both new and missing responses, smallest $t(240) = 3.11$, $p = .01$. $d = 0.56$. There was no significant difference between the latter responses, $t(240) = 0.77$, $p = .87$, $d = 0.14$. These results suggest that recognition accuracy was comparable recognition for both age groups. This interpretation was supported by the results of a model comparing the bias-corrected traditional recognition index between age groups that showed (Figure 2B) no significant age difference, $t(60) = 0.19$, $p = .85$, $d = 0.05$. Taken together, the MST results replicated earlier findings showing selective age-related deficits in mnemonic discrimination.

Perceptual Discrimination Task. *No Age Differences in Perceptual Discrimination.* Perceptual discrimination of similar objects was assessed to examine whether age-related deficits in LDI scores reflected a perceptual deficit. For completeness, Table 4 displays all response probabilities on the PDT. Given our primary interest in mnemonic and perceptual discrimination of similar objects, we focused on bias-corrected responses for those objects (Figure 2C). We created a perceptual discrimination index (PDI) by computing the difference in similar responses for similar and different objects [p(similar | similar objects) – p(similar | different objects)]. A model comparing PDI scores for younger and older adults indicated no significant difference, $t(60) = 0.12$, $p = .90$, $d = .03$, suggesting that older adults' lower LDI scores primarily reflected an age-related deficit in mnemonic rather than perceptual processes.

Results from Connectome-based Predictive Modeling.

Statistical Approach for Generating a Connectivity Matrix. CPM models were estimated using the *NetworkToolbox* package (version 1.4.2; 57) in R software. CPM constructs a connectome that is significantly associated with a behav-

Table 4. Response Probabilities on the Perceptual Discrimination Task

	Object Type					
	Same Objects		Similar Objects		Different Objects	
Response	Younger	Older	Younger	Older	Younger	Older
Same	.93 [.91, .94]	.93 [.91, .95]	.08 [.05, .10]	.09 [.06, .12]	.01 [.00, .03]	.01 [.00, .03]
Similar	.07 [.05, .09]	.06 [.05, .09]	.88 [.86, .91]	.85 [.82, .88]	.05 [.03, .07]	.02 [.00, .04]
Different	.00 [.00, .00]	.01 [.00, .03]	.04 [.01, .06]	.06 [.03, .09]	.94 [.92, .96]	.97 [.95, .99]

Note. 95% confidence intervals are displayed in brackets.

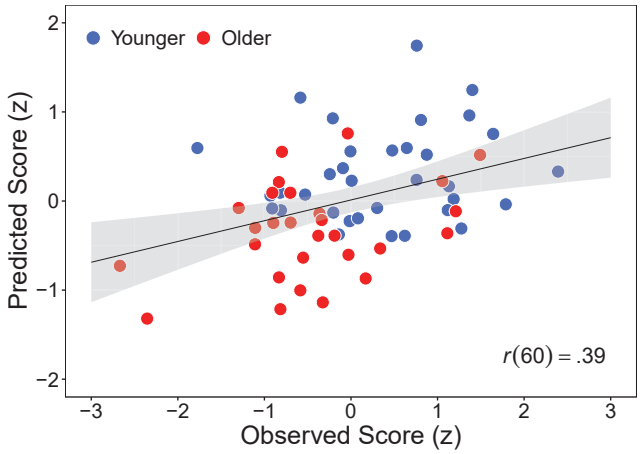

Fig. 3. Intrinsic Default Mode Network Connectivity Predicting Mnemonic Discrimination. A scatterplot showing the association between predicted and observed Lure Discrimination Index scores (standardized) based on the Mnemonic Discrimination Connectome for younger (blue) and older (red) adults. Points are individual participants, the line is the best fitting regression line, and the shaded region is the 95% confidence interval.

ioral measure via a leave-one-out cross-validation approach (e.g., 58). Each behavioral measure used in CPM generates a specific connectome. Here, we generated a connectome for mnemonic discrimination using the LDI score as the behavioral measure. Each participant's resting-state data comprised the functional connectivity matrix of ROIs described above, henceforth referred to as ROI–ROI matrices. The CPM approach proceeded as follows. First, the ROI–ROI matrix and mnemonic discrimination for one participant (i.e., the test participant) was separated from the remaining participants (i.e., training participants). The training participants' ROI–ROI matrices were then used to correlate each ROI–ROI element across the matrices with their respective mnemonic discrimination performance. To rule out artifactual relationships from age-related structural brain differences, intracranial volume (total volume including gray matter, white matter, and CSF) was controlled when computing correlations between ROI–ROI elements and mnemonic discrimination. These correlations formed a single correlation matrix thresholded at $\alpha = .05$ (30).

Next, the thresholded matrix was separated into two masks that comprised only significant positive or negative correlations. Creating these separate positive and negative masks allowed us to dissociate connectivity patterns that were positively and negatively associated with mnemonic discrimination. Each mask was separately applied to each training participant's ROI–ROI matrix, leaving only the connectivity values that were significantly related to behavioral performance. For each participant, sum totals of these remaining connectivity values were calculated for each mask. Then, these sum totals were entered into separate regression models to predict the training participants' mnemonic discrimination.

The regression weights from these models were then used to predict the test participant's mnemonic discrimination. Using the test participant's ROI–ROI matrix, sum scores from the positive and negative masks were computed to estimate mnemonic discrimination for the test participant by solving the respective regression equations. The predicted LDI value from the positive mask is referred to as the positive prediction, and the predicted LDI value from the negative mask is referred to as the negative prediction. This process repeated until all participants served once as the test participant, thus producing two predicted LDI values per participant. Finally, the connectome-predicted and observed LDI values were correlated. A significant correlation indicates that a set of connected ROIs (i.e., connectome) had sufficient explanatory power for mnemonic discrimination performance.

DMN Connectivity and Mnemonic Discrimination. To test our primary hypothesis that DMN connectivity should predict mnemonic discrimination, we used CPM to correlate predicted with observed LDI scores. Supporting our hypothesis, the positive prediction model was significant, $r(60) = .39$, $p < .01$ (see Figure 3), and 209 out of 903 possible connections (23%) significantly predicted mnemonic discrimination. This effect size was comparable to those reported in previous studies using CPM to predict behavior from intrinsic connectivity (e.g., 59). Because leave-one-out connectome estimations are not independent, a permutation test was performed to assess the likelihood that the positive prediction model emerged by chance. A null distribution was created by randomly shuffling observed LDI scores, re-running CPM, and computing 1000 correlations between predicted and observed scores. There was a significant difference between the null and positive prediction models, $p < .01$, indicating that the positive prediction model was unlikely to have emerged by chance. The negative prediction model, which was not significant, $r(60) = -.23$, $p = .08$, included 22 out of 903 possible significant connections (2%) and is not considered further.

The connections among regions in the positive prediction model, hereafter referred to as the Mnemonic Discrimination Connectome (MDC), are displayed in Figure 4 (glass brain format) and Figure **??**A (grid format). To summarize the locations of these connections, we computed the proportion of connections out of all possible connections within and between four major regions (i.e., prefrontal, hippocampus, temporal, and parietal). In this approach, each proportion is independent of the others. These summaries (Figure 6, top panels) indicate that the relative proportion of connections was greatest within the temporal cortex (panel A) and between the temporal cortex and other regions (panel B). Thus, the temporal regions of the DMN were the most densely connected in the MDC.

Hippocampal Connectivity in the MDC. As described in the Introduction, the MST has primarily been used to examine the relationship between hippocampal function and mnemonic discrimination. To highlight the connectivity involving the hippocampus in the MDC, we explored the inter-region connections originating from the head, body, and tail of the hippocampus in both hemispheres (Figure 8). Within

the MDC, the connectivity was greatest for the left hippocampal head with 11 connections and the right hippocampal body region with 10 connections. Across all divisions of the hippocampus, most connections were found in temporal (14) and prefrontal (13) regions.

To establish the specificity of the MDC, we examined whether intrinsic DMN connectivity selectively predicted mnemonic discrimination. If the MDC is specifically related to performance on the measure assessing the mechanisms supporting mnemonic discrimination, then the MDC should not predict performance on measures supported by non-identical mechanisms. Consistent with this assertion, Figure 7 (top panels) shows that the MDC did not significantly predict scores on indices of recognition memory (r = -0.18, p = .15, panel A) or perceptual discrimination (r = 0.11, p = .39, panel B). We also conducted a more conservative test of MDC selectivity by applying CPM to recognition and perceptual discrimination scores to establish whether a behavior-specific connectome could be identified for such indices. Given that we focused primarily on the significant positive prediction model for LDI scores (i.e., the MDC), we focus here only on positive prediction models for recognition and perceptual discrimination. Figure 7 (bottom panels) shows that connectomes built from intrinsic DMN connectivity did not have sufficient explanatory power to predict scores on recognition (r = -0.01, p = .93, panel C) or perceptual discrimination (r = 0.10, p = .43, panel D) indices. These results indicate that intrinsic DMN connectivity selectively predicted mnemonic discrimination.

Age Differences in MDC Connection Strength. The second aim of the present study was to examine if intrinsic DMN connectivity in the CPM would positively predict mnemonic discrimination more strongly for younger than older adults. We tested for such differences by summing all MDC connections and comparing those values between age groups with a two-sample t-test. This measure of connection strength was significantly greater for younger (M = 54.05, SD = 12.78) than older (M = 36.83, SD = 14.56) adults, $t(60)$ = 4.96, p < .001, d = 1.26. To determine if this difference was due to chance, we performed a permutation test. We first created a null distribution of t-statistics based on strength differences between age groups by computing 1000 random connectomes with ROIs including the original MDC connections. The t-statistic from the MDC (4.96) was well beyond the upper bound of the null distribution (range = 3.64–4.63, M = 4.12, SD = 0.19), suggesting that younger adults' greater connection strength was unlikely due to chance.

To identify the locations of age differences in the MDC, we used two-sample t-tests to compare the strength of each ROI–ROI connection between age groups (Figure **??**B). Out of the 209 possible MDC connections, 22 (11%) showed greater strength for younger than older adults and survived false discovery rate correction. These stronger connections for younger adults were most prominently located within the temporal cortex (Figure 6C) and between the temporal and prefrontal cortex (Figure 6D).

Finally, the age differences in MDC connectivity strength shown here may have partly reflected stronger baseline DMN connectivity for younger than older adults, as such age differences have been shown in earlier studies (e.g., 21). Consistent with this possibility, we identified a role for DMN connectivity strength in age-related MDC connectivity differences by comparing ROI–ROI connection strength in the DMN between age groups (Figure 3C). Younger adults showed significantly stronger average connectivity that survived false discover rate correction in 62 connections between regions across the DMN (cells with thick borders). Of these differences, 22 (35.5%) were connections within the MDC (Figure 3B). These results suggest that younger adults' stronger baseline DMN connectivity partly contributed to their stronger connectivity among regions that predict mnemonic discrimination.

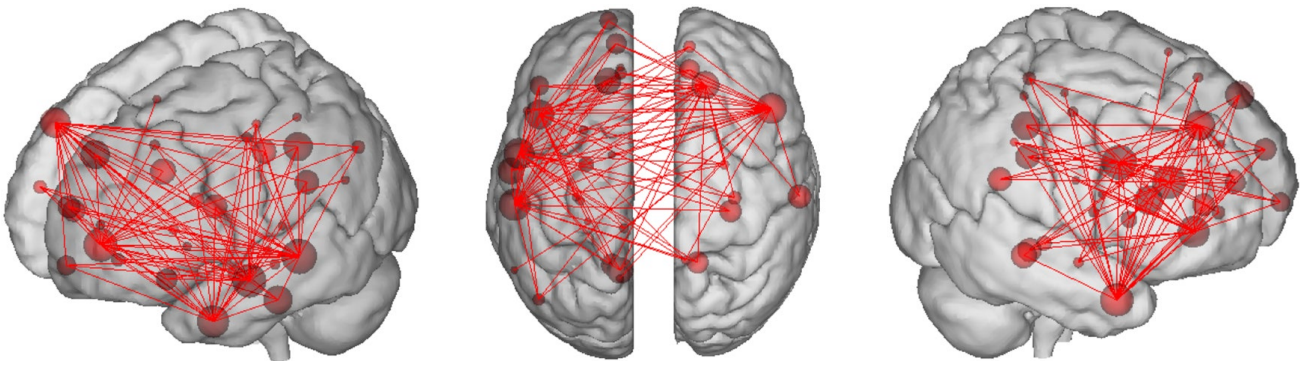

Fig. 4. Connections in the Mnemonic Discrimination Connectome (MDC). The MDC visualized from three orientations (left, top, right) using the BioImage Suite Web Viewer: https://bioimagesuiteweb.github.io/webapp/connviewer.html. To provide an interpretable connectome, the threshold for including regions of interest here was set at 20 or more connections. Images using other thresholds can be generated using the data provided on the OSF: https://osf.io/f6vg8/. Larger node sizes (circles) indicate more inter-regional connections (lines).

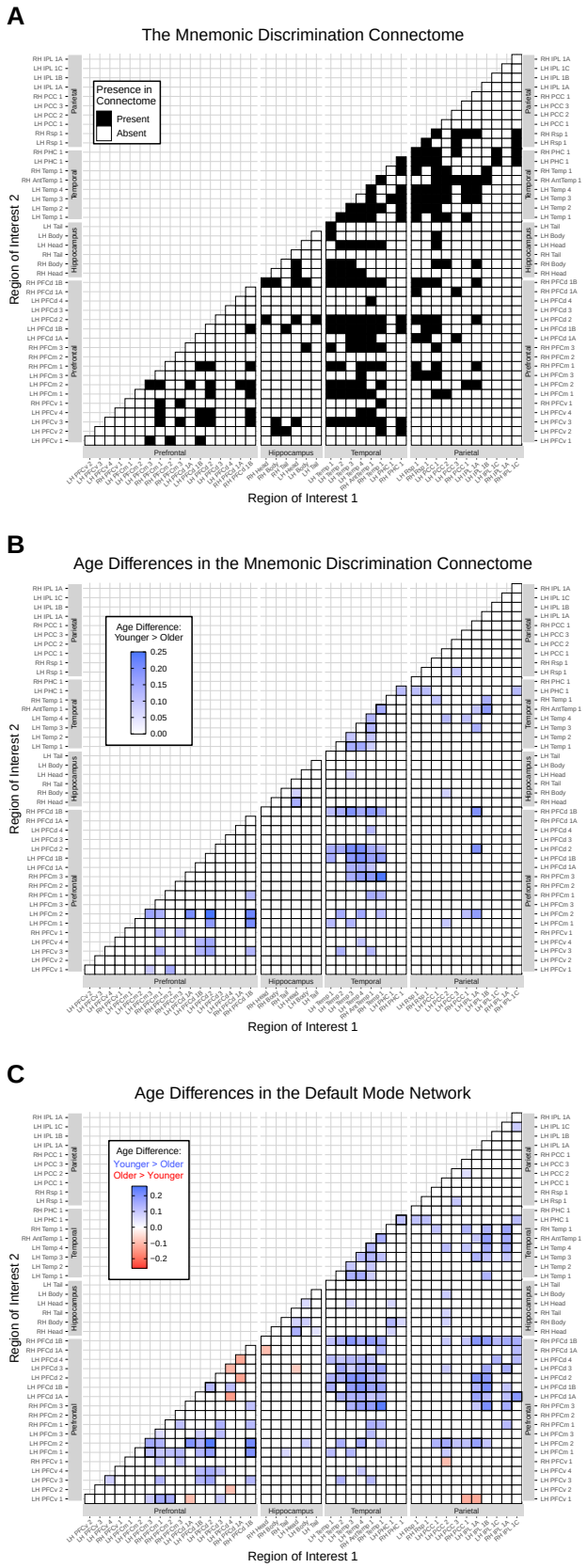

Fig. 5. Inter-Regional Connections. (A) The significant connections among regions of interest (ROIs) in the Default Mode Network (DMN) identified in the Mnemonic Discrimination Connectome (MDC). ROI–ROI connections were present in (black squares) or absent from (white squares) the MDC. (B) Age differences in MDC connections. Blue squares show ROI–ROI connections that were stronger for younger than older adults. Connections that were significantly different between age groups and survived False Discovery Rate (FDR) correction are indicated by thicker black borders. (C) Age differences in DMN connections. Blue squares show ROI–ROI connections that were stronger for younger than older adults; red squares show greater connectivity for older than younger adults. Connections that were significantly different between age groups and survived False Discovery Rate (FDR) correction are indicated by thicker black borders. B and C) The color intensities of grid squares indicate the degree of average differences in correlations between Lure Discrimination Index scores and ROI–ROI connections between younger and older adults. (All Panels) ROIs are ordered anterior to posterior starting from the left (x-axis) and bottom (y-axis). Axis labels correspond to the codes in Table 2.

Discussion

Discriminating existing memories from similar perceptual inputs to mitigate interference is a core feature of episodic memory. Although studies examining the neural mechanisms of mnemonic discrimination have focused primarily on hippocampal structure and function (for a review, see 4), mounting evidence suggests that regions beyond the hippocampus also support this ability (10, 14, 16, 19). The present study extends this nascent literature by characterizing the relationship between functional connectivity among DMN regions and mnemonic discrimination ability. Using a data-driven connectomics approach (30), we showed that inter-individual differences in intrinsic connectivity among regions in the DMN predicted mnemonic discrimination. This relationship primarily involved connections with temporal cortex. Further, the better discrimination shown by younger than older adults were primarily reflected in areas where younger adults had stronger temporal-prefrontal connectivity than older adults. These results provide evidence that mnemonic discrimination is supported by connectivity across DMN regions including, but not limited to, the hippocampus. The predictive relationship between DMN connectivity and mnemonic discrimination is consistent with results suggesting that such connectivity supports episodic memory functions (21, 22). DMN subregions, such as medial prefrontal and temporopolar cortex, are presumably involved in mnemonic functions (23, 24). Consistent with these findings, the current study showed that connectivity between such regions predicted mnemonic discrimination. In fact, connections positively related to mnemonic discrimination were broadly distributed across prefrontal, hippocampal, temporal, and parietal regions. These findings suggest that broad cortical connections support mnemonic functions that have often been attributed to hippocampal and adjacent connections in the medial temporal lobes (for a review, see 4). Most of the predictive connections within and between these regions emerged within temporal cortex between regions around the temporal pole. The observed associations between anterior temporal connections and mnemonic discrimination is remi-

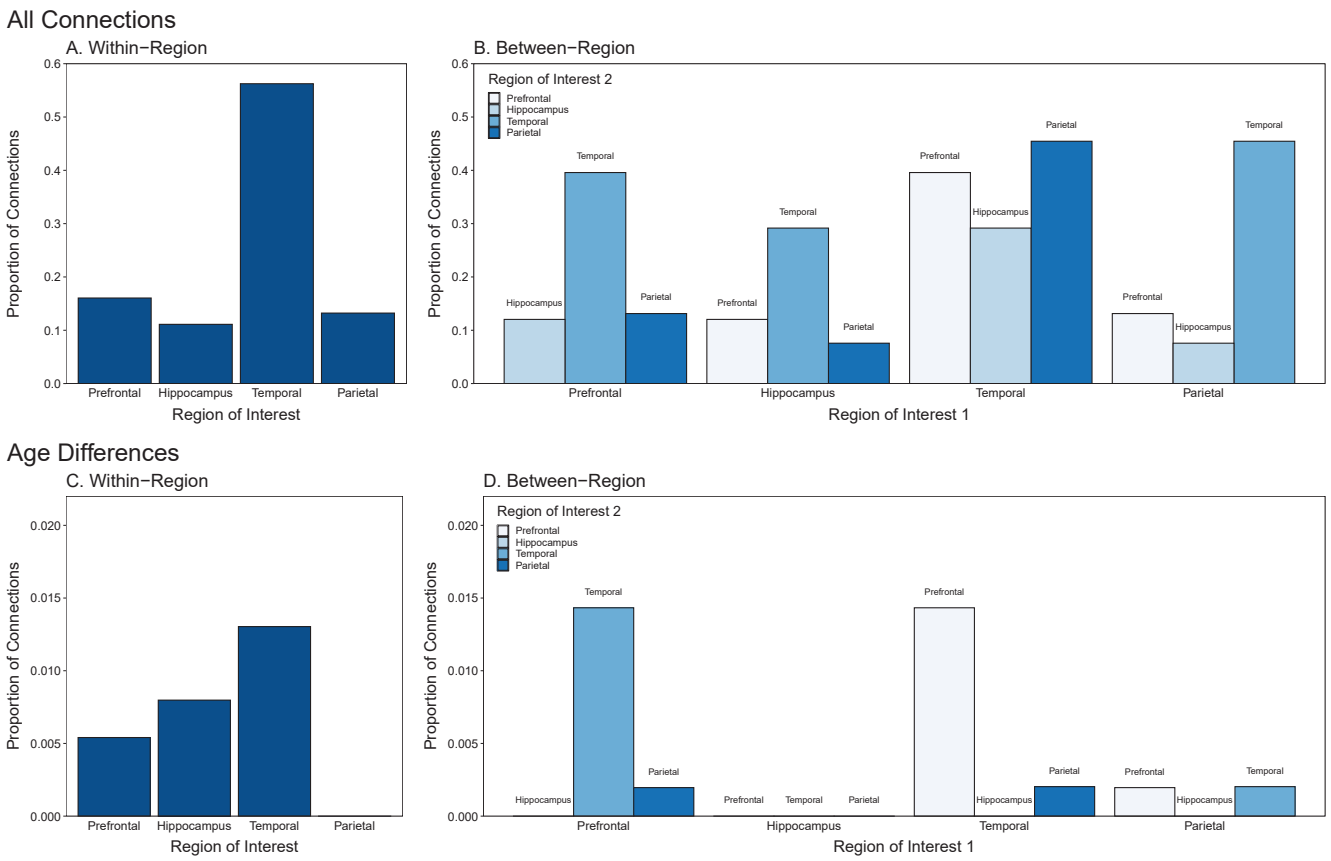

Fig. 6. Proportions of Connections in the Major Regions of the Mnemonic Discrimination Connectome. (Top panel) Total proportions of connections within (A) and between (B) regions. (Bottom panel) Proportions of regions showing significantly greater connectivity for younger than older adults that survived false discovery rate correction (C) within and (D) between regions. Proportions were computed separately within each region and between each pair of regions using the total unique number of possible connections in each as the denominator. Therefore, the values above are independent of each other and can all range from 0–1.0.

niscent of findings showing that anterior temporal activity is involved in storing semantic representations (60). Relatedly, people with atrophy near and around the temporal pole show difficulty naming and recognizing everyday objects (61, 62). The present findings suggest that the strength of intrinsic DMN connections involving anterior temporal cortex may support the ability to distinguish between everyday objects.

The greater connectivity strength of predictive connections within more anterior DMN regions also complements theoretical accounts positing that an anterior-temporal DMN subnetwork preferentially supports memory for local items or objects (13, 20, 63, 64). This anterior DMN emphasis in the MDC is further qualified by the greater number of significant connections observed in anterior portions of the hippocampus. The present data support the growing perspective that hippocampal pattern separation processes likely interact with cortical processes to support mnemonic discrimination. Consistent with this perspective, weaker functional connectivity between the anterior hippocampus and parahippocampal cortex during MST performance has been associated with poorer mnemonic discrimination in older adults (29). However, unlike many prior results, the present findings suggest that intrinsic relationships among DMN regions, even at rest, predict the ability to discriminate similar inputs and mitigate subsequent interference. The prominent anterior cortical connections in the MDC suggest that functional interactions between anterior temporal and prefrontal regions may play critical roles in mnemonic discrimination ability and have important interactions with anterior portions of the hippocampus. The nature and extent of these relationships should be explored in future studies of mnemonic discrimination.

It is also noteworthy that although DMN connections predicted mnemonic discrimination, they did not predict perceptual discrimination or traditional recognition. The absence of DMN connections predicting perceptual discrimination suggests more specific DMN involvement in episodic memory operations than in visual detection of perceptual differences between objects. However, given that traditional recognition is clearly an aspect of episodic memory, it may seem surprising that DMN connections did not predict that ability. However, the processes involved in mnemonic discrimination and traditional recognition are not identical, suggesting that specific types of episodic memory processes are supported by intrinsic DMN connectivity. Indeed, the exact neural mechanisms underlying these memory processes are likely distinct (65). One possibility to be explored in future research is whether intrinsic connections between the DMN and other brain networks predict traditional recognition. Consistent

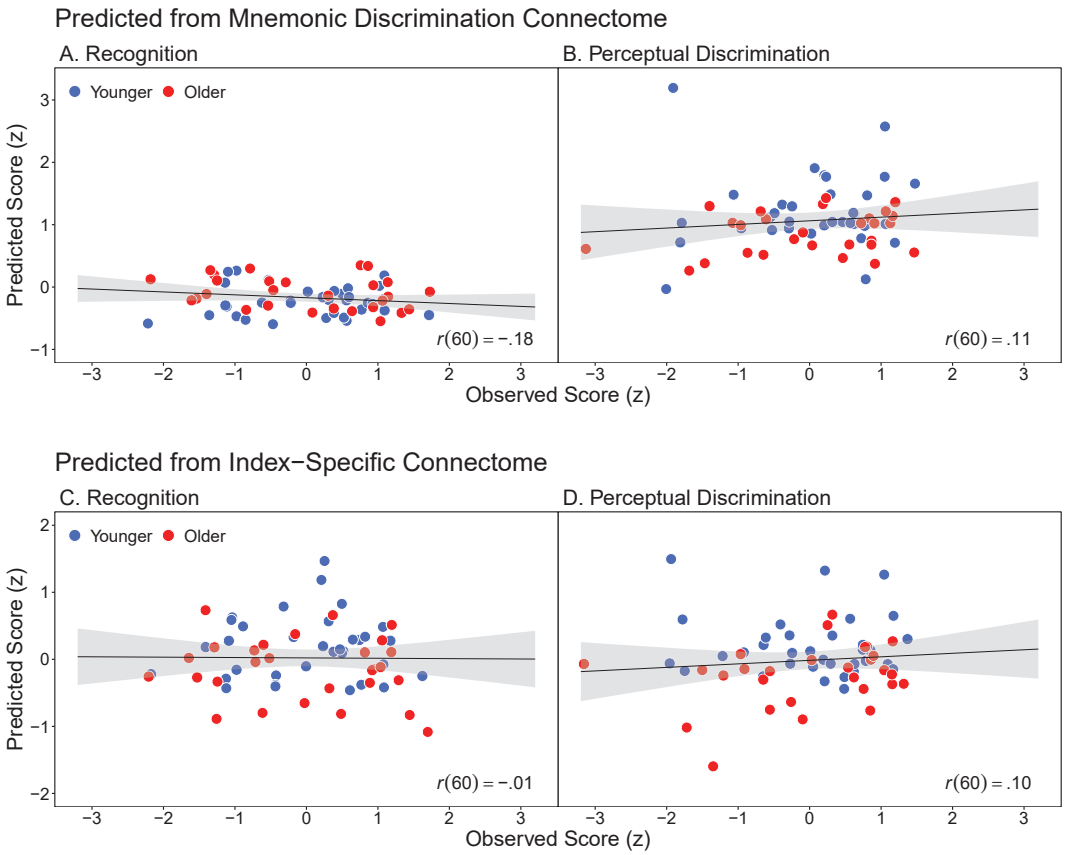

Fig. 7. Intrinsic Functional Connectivity Predicting Recognition and Perceptual Discrimination. Scatterplots showing the association between predicted and observed Traditional Recognition (A and C) and Perceptual Discrimination Index (B and D) scores (standardized). (Top panel) Associations including predicted scores based on the Mnemonic Discrimination Connectome. (Bottom panel) Associations including predicted scores based on connectomes created for recognition and perceptual discrimination based on intrinsic Default Mode Network connectivity. Points are individual participants (younger = blue; older = red), the lines are the best fitting regression lines, and the shaded regions are 95% confidence intervals.

with this possibility, intra-network connections have been linked to cognitive abilities (66).

As stated above, the present study is the first to our knowledge to use a network-based approach to identify the neural mechanisms supporting mnemonic discrimination. The CPM approach enabled exploratory analyses extending beyond traditional whole-brain activation patterns. Although CPM is usually applied to whole-brain connectivity (30), we took a more targeted approach motivated by prior research to examine functional connectivity among DMN regions including the hippocampus. This reduced the number of ROIs in the connectome and allowed for more precise inferences, such as identifying age differences in mnemonic discrimination ability predicted by connectivity in anterior, medial, and posterior regions of the DMN.

The present study was also the first examine adult age differences in an aspect of episodic memory using CPM. Here, the predictive strength of the MDC was greater for younger than older adults. This suggests that older adults have less defined DMN co-activation predicting mnemonic discrimination. Older adults also showed weaker overall baseline DMN connectivity than younger adults, including the connections in the MDC. Weakened or dysfunctional circuitry among DMN regions in older adults is associated with episodic memory deficits (37) and more specific age-related deficits in mnemonic discrimination (3, 13, 27, 28). Thus, the present findings suggest that lower network cohesion at baseline may be less predictive of behavior under the CPM approach.

Relatedly, CPM can also detect cognitive impairments associated with Alzheimer's disease in intrinsic whole-brain connectivity (67). Similarly, the MDC reported here identified activation patterns associated with age-related deficits in mnemonic discrimination of visual objects. Given that impaired visual object discrimination is associated with mild cognitive impairment and Alzheimer's disease (68) as well as beta-amyloid protein deposition, which is an earlier indicator of Alzheimer's disease pathology (69), the MDC may predict pathological brain changes. If so, the MDC could serve as a biomarker of normal and pathological cognitive decline. Future research could examine if the MDC predicts Alzheimer's risk in older adults, potentially providing an early indicator of eventual conversion. This direction is especially promising if neural predictors of mnemonic discrimination ability can be obtained from brief resting-state scans.

There were some limitations in the present study. First, resting-state functional connectivity data is susceptible to contamination from uncontrolled sources of variability (e.g., participant respiration). We accounted for this using a con-

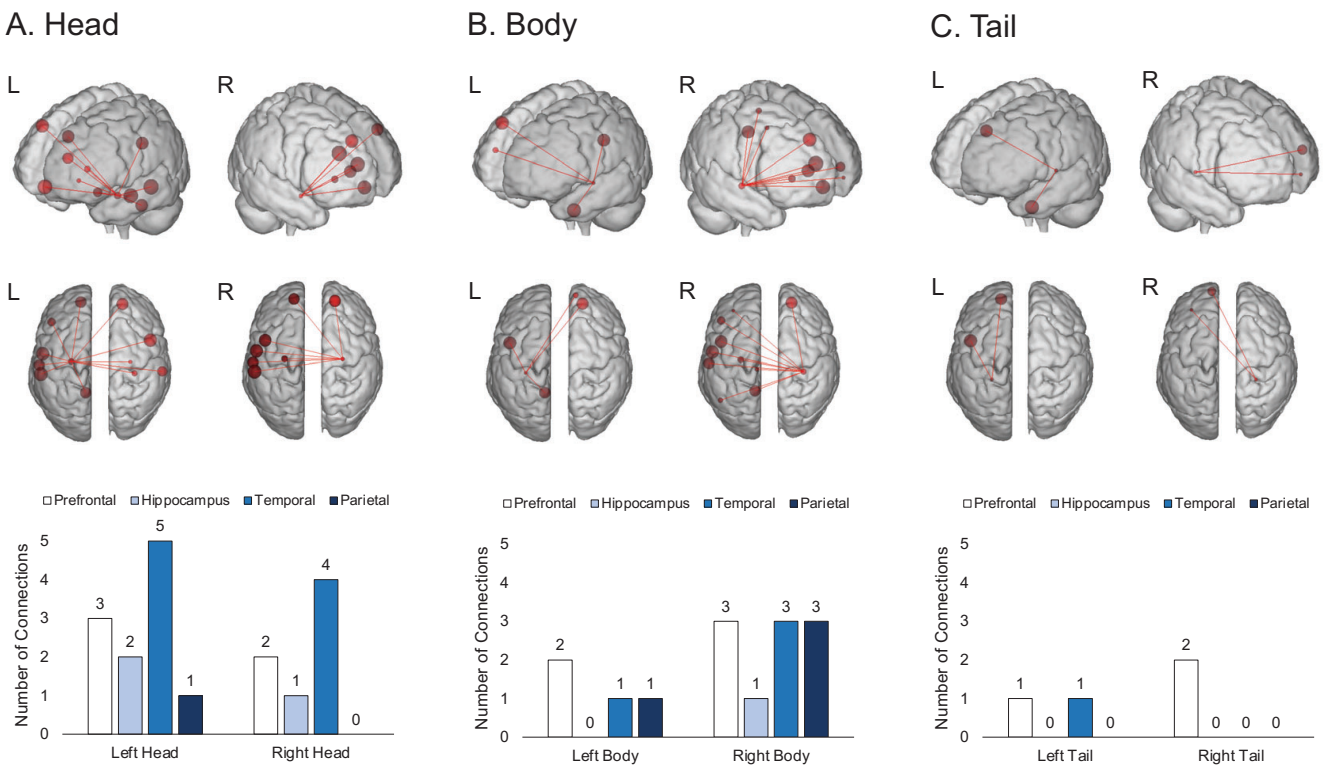

Fig. 8. Inter-Region Connectivity from Regions of the Hippocampus in the Mnemonic Discrimination Connectome (MDC). (Top two rows) Connections from the hippocampal head (A), body (B), and tail (C) visualized using the BioImage Suite Web Viewer: https://bioimagesuiteweb.github.io/webapp/connviewer.html. The threshold for including regions of interest here was set at one or more connections. Images using other thresholds can be generated using the data provided on the OSF: https://osf.io/f6vg8/. Larger node sizes (circles) indicate more connections (lines) from each hippocampal region to others in the MDC. (Bottom row) Summaries displaying the numbers of connections from each hippocampal region.

servative preprocessing method that partly controls for such variability (47), but future work could also include physiological measures as regressors in comparable analyses. Second, the extreme groups design precluded causal inferences from age-related effects. Third, although the current sample sizes are comparable to related work (17), more reliable estimates between intrinsic connectivity and behavior can be derived from larger samples (70, 71). Despite these limitations, the present findings are consistent with work showing age differences in mnemonic discrimination (for a review, see 4) and DMN contributions to episodic memory (21).

In sum, the present study was the first to leverage a connectomics approach to examine the association between individual variation in intrinsic functional connectivity among DMN regions and mnemonic discrimination of visual objects in younger and older adults. The connectome established here showed that connections within and between temporal, prefrontal, parietal, and hippocampal regions at rest predicted mnemonic discrimination ability. Such relationships indicate clearly that a comprehensive explanation of the neural mechanisms of mnemonic discrimination requires widening the focus beyond the medial temporal lobes and adjacent subcortical structures to examine broader cortical networks including those structures.

ACKNOWLEDGEMENTS

This project received funding from the Scientific Research Network on Decision Neuroscience and Aging (NIA R24-AG054355). The stimuli, data, and analysis scripts are available on the Open Science Framework: https://osf.io/f6vg8/.

Bibliography

1. Kenneth A. Norman and Randall C. O'Reilly. Modeling hippocampal and neocortical contributions to recognition memory: A complementary-learning-systems approach. 110(4): 611–646. ISSN 0033-295X. doi: 10.1037/0033-295X.110.4.611. Publisher: American Psychological Association.
2. Randall C. O'Reilly and James L. McClelland. Hippocampal conjunctive encoding, storage, and recall: Avoiding a tradeoff. 4(6):661–682. ISSN 1050-9631, 1098-1063. doi: 10.1002/hipo.450040605.
3. Michael A. Yassa and Craig E. L. Stark. Pattern separation in the hippocampus. 34(10):515–525. ISSN 01662236. doi: 10.1016/j.tins.2011.06.006.
4. Shauna M. Stark, C. Brock Kirwan, and Craig E.L. Stark. Mnemonic similarity task: A tool for assessing hippocampal integrity. 23(11):938–951, . ISSN 13646613. doi: 10.1016/j.tics.2019.08.003.
5. A. Bakker, C. B. Kirwan, M. Miller, and C. E. L. Stark. Pattern separation in the human hippocampal CA3 and dentate

gyrus. 319(5870):1640–1642, . ISSN 0036-8075, 1095-9203. doi: 10.1126/science.1152882.
6. D. Berron, H. Schutze, A. Maass, A. Cardenas-Blanco, H. J. Kuijf, D. Kumaran, and E. Duzel. Strong evidence for pattern separation in human dentate gyrus. 36(29):7569–7579. ISSN 0270-6474, 1529-2401. doi: 10.1523/JNEUROSCI.0518-16.2016.
7. C. B. Kirwan and C. E.L. Stark. Overcoming interference: An fMRI investigation of pattern separation in the medial temporal lobe. 14(9):625–633. ISSN 1072-0502. doi: 10.1101/lm.663507.
8. K. F. LaRocque, M. E. Smith, V. A. Carr, N. Witthoft, K. Grill-Spector, and A. D. Wagner. Global similarity and pattern separation in the human medial temporal lobe predict subsequent memory. 33(13):5466–5474. ISSN 0270-6474, 1529-2401. doi: 10.1523/JNEUROSCI.4293-12.2013.
9. Marwa Azab, Shauna M. Stark, and Craig E.L. Stark. Contributions of human hippocampal subfields to spatial and temporal pattern separation: Domain agnostic role for the dentate gyrus. 24(3):293–302. ISSN 10509631. doi: 10.1002/hipo.22223.
10. Zachariah M. Reagh, Jared M. Roberts, Maria Ly, Natalie DiProspero, Elizabeth Murray, and Michael A. Yassa. Spatial discrimination deficits as a function of mnemonic interference in aged adults with and without memory impairment. 24(3):303–314, . ISSN 10509631. doi: 10.1002/hipo.22224.
11. Caitlin R. Bowman and Nancy A. Dennis. The neural basis of recollection rejection: Increases in hippocampal–prefrontal connectivity in the absence of a shared recall-to-reject and target recollection network. 28(8):1194–1209. ISSN 0898-929X, 1530-8898. doi: 10.1162/jocn_a_00961.
12. S. E. Motley and C. B. Kirwan. A parametric investigation of pattern separation processes in the medial temporal lobe. 32(38):13076–13084. ISSN 0270-6474, 1529-2401. doi: 10.1523/JNEUROSCI.5920-11.2012.
13. Zachariah M. Reagh, Jessica A. Noche, Nicholas J. Tustison, Derek Delisle, Elizabeth A. Murray, and Michael A. Yassa. Functional imbalance of anterolateral entorhinal cortex and hippocampal dentate/CA3 underlies age-related object pattern separation deficits. 97(5):1187–1198.e4, . ISSN 08966273. doi: 10.1016/j.neuron.2018.01.039.
14. Peter E. Wais, Sahar Jahanikia, Daniel Steiner, Craig E.L. Stark, and Adam Gazzaley. Retrieval of high-fidelity memory arises from distributed cortical networks. 149:178–189. ISSN 10538119. doi: 10.1016/j.neuroimage.2017.01.062.
15. Meera Paleja, Todd A. Girard, Katherine A. Herdman, and Bruce K. Christensen. Two distinct neural networks functionally connected to the human hippocampus during pattern separation tasks. 92:101–111. ISSN 02782626. doi: 10.1016/j.bandc.2014.10.009.
16. Laura M. Pidgeon and Alexa M. Morcom. Cortical pattern separation and item-specific memory encoding. 85:256–271. ISSN 00283932. doi: 10.1016/j.neuropsychologia.2016.03.026.
17. Jenna L. Klippenstein, Shauna M. Stark, Craig E. L. Stark, and Ilana J. Bennett. Neural substrates of mnemonic discrimination: A whole-brain fMRI investigation. 10(3). ISSN 2162-3279, 2162-3279. doi: 10.1002/brb3.1560.
18. Marcus E. Raichle. The brain's default mode network. 38 (1):433–447. ISSN 0147-006X, 1545-4126. doi: 10.1146/annurev-neuro-071013-014030.
19. Michelle I Nash, Cooper B Hodges, Nathan M Muncy, and C Brock Kirwan. Pattern separation beyond the hippocampus: A high-resolution whole-brain investigation of mnemonic discrimination in healthy adults. 31(4):408–421.
20. Sarah A. Johnson, Sabrina Zequeira, Sean M. Turner, Andrew P. Maurer, Jennifer L. Bizon, and Sara N. Burke. Rodent mnemonic similarity task performance requires the prefrontal cortex. page hipo.23316. ISSN 1050-9631, 1098-1063. doi: 10.1002/hipo.23316.
21. Jessica R. Andrews-Hanna, Jay S. Reidler, Jorge Sepulcre, Renee Poulin, and Randy L. Buckner. Functional-anatomic fractionation of the brain's default network. 65(4):550–562, . ISSN 08966273. doi: 10.1016/j.neuron.2010.02.005.
22. R. Nathan Spreng and Cheryl L. Grady. Patterns of brain activity supporting autobiographical memory, prospection, and theory of mind, and their relationship to the default mode network. 22(6):1112–1123. ISSN 0898-929X, 1530-8898. doi: 10.1162/jocn.2009.21282.
23. Hongkeun Kim. Default network activation during episodic and semantic memory retrieval: A selective meta-analytic comparison. 80:35–46. ISSN 00283932. doi: 10.1016/j.neuropsychologia.2015.11.006.
24. C. Sestieri, M. Corbetta, G. L. Romani, and G. L. Shulman. Episodic memory retrieval, parietal cortex, and the default mode network: Functional and topographic analyses. 31(12):4407–4420. ISSN 0270-6474, 1529-2401. doi: 10.1523/JNEUROSCI.3335-10.2011.
25. Willem Huijbers, Cyriel M. A. Pennartz, Roberto Cabeza, and Sander M. Daselaar. The hippocampus is coupled with the default network during memory retrieval but not during memory encoding. 6(4):e17463. ISSN 1932-6203. doi: 10.1371/journal.pone.0017463.
26. Shauna M. Stark, Michael A. Yassa, Joyce W. Lacy, and Craig E.L. Stark. A task to assess behavioral pattern separation (BPS) in humans: Data from healthy aging and mild cognitive impairment. 51(12):2442–2449, . ISSN 00283932. doi: 10.1016/j.neuropsychologia.2012.12.014.
27. Arnold Bakker, Gregory L. Krauss, Marilyn S. Albert, Caroline L. Speck, Lauren R. Jones, Craig E. Stark, Michael A. Yassa, Susan S. Bassett, Amy L. Shelton, and Michela Gallagher. Reduction of hippocampal hyperactivity improves cognition in amnestic mild cognitive impairment. 74(3):467–474, . ISSN 08966273. doi: 10.1016/j.neuron.2012.03.023.
28. Michael A. Yassa, Joyce W. Lacy, Shauna M. Stark, Marilyn S. Albert, Michela Gallagher, and Craig E.L. Stark. Pattern separation deficits associated with increased hippocampal CA3 and dentate gyrus activity in nondemented older adults. pages n/a–n/a. ISSN 10509631. doi: 10.1002/hipo.20808.
29. Shauna M Stark, Amy Frithsen, and Craig E L Stark. Age-related alterations in functional connectivity along the longitudinal axis of the hippocampus and its subfields. *Hippocampus*, 31(1):11–27, 2021. doi: 10.1002/hipo.23259.
30. Xilin Shen, Emily S Finn, Dustin Scheinost, Monica D Rosenberg, Marvin M Chun, Xenophon Papademetris, and R Todd Constable. Using connectome-based predictive modeling to predict individual behavior from brain connectivity. 12(3):506–518. ISSN 1754-2189, 1750-2799. doi: 10.1038/nprot.2016.178.
31. Monica D Rosenberg, Emily S Finn, Dustin Scheinost, Xenophon Papademetris, Xilin Shen, R Todd Constable, and Marvin M Chun. A neuromarker of sustained attention

from whole-brain functional connectivity. 19(1):165–171, . ISSN 1097-6256, 1546-1726. doi: 10.1038/nn.4179.
32. Monica D. Rosenberg, Wei-Ting Hsu, Dustin Scheinost, R. Todd Constable, and Marvin M. Chun. Connectome-based models predict separable components of attention in novel individuals. 30(2):160–173, . ISSN 0898-929X, 1530-8898. doi: 10.1162/jocn_a_01197.
33. Roger E. Beaty, Yoed N. Kenett, Alexander P. Christensen, Monica D. Rosenberg, Mathias Benedek, Qunlin Chen, Andreas Fink, Jiang Qiu, Thomas R. Kwapil, Michael J. Kane, and Paul J. Silvia. Robust prediction of individual creative ability from brain functional connectivity. 115(5):1087–1092. ISSN 0027-8424, 1091-6490. doi: 10.1073/pnas.1713532115.
34. Wei-Ting Hsu, Monica D Rosenberg, Dustin Scheinost, R Todd Constable, and Marvin M Chun. Resting-state functional connectivity predicts neuroticism and extraversion in novel individuals. 13(2):224–232. ISSN 1749-5016, 1749-5024. doi: 10.1093/scan/nsy002.
35. Stephanie Fountain-Zaragoza, Shaadee Samimy, Monica D. Rosenberg, and Ruchika Shaurya Prakash. Connectome-based models predict attentional control in aging adults. 186:1–13. ISSN 10538119. doi: 10.1016/j.neuroimage.2018.10.074.
36. Jessica R. Andrews-Hanna, Abraham Z. Snyder, Justin L. Vincent, Cindy Lustig, Denise Head, Marcus E. Raichle, and Randy L. Buckner. Disruption of large-scale brain systems in advanced aging. 56(5):924–935, . ISSN 08966273. doi: 10.1016/j.neuron.2007.10.038.
37. Adam M. Staffaroni, Jesse A. Brown, Kaitlin B. Casaletto, Fanny M. Elahi, Jersey Deng, John Neuhaus, Yann Cobigo, Paige S. Mumford, Samantha Walters, Rowan Saloner, Anna Karydas, Giovanni Coppola, Howie J. Rosen, Bruce L. Miller, William W. Seeley, and Joel H. Kramer. The longitudinal trajectory of default mode network connectivity in healthy older adults varies as a function of age and is associated with changes in episodic memory and processing speed. 38(11):2809–2817. ISSN 0270-6474, 1529-2401. doi: 10.1523/JNEUROSCI.3067-17.2018.
38. Ziad S. Nasreddine, Natalie A. Phillips, ValÃ©rie BÃ©dirian, Simon Charbonneau, Victor Whitehead, Isabelle Collin, Jeffrey L. Cummings, and Howard Chertkow. The montreal cognitive assessment, MoCA: A brief screening tool for mild cognitive impairment. 53(4):695–699. ISSN 00028614, 15325415. doi: 10.1111/j.1532-5415.2005.53221.x.
39. D. Wechsler. *Wechsler Memory Scale–Third Edition*. The Psychological Corporation.
40. R. A. Zachary and W. C. Shipley. *Shipley institute of living scale: Revised Manual*. Western Psychological Services.
41. Trey Hedden, Denise C. Park, Richard Nisbett, Li-Jun Ji, Qicheng Jing, and Shulan Jiao. Cultural variation in verbal versus spatial neuropsychological function across the life span. 16(1):65–73. ISSN 0894-4105. doi: 10.1037//0894-4105.16.1.65.
42. E-prime 3.0.
43. Patrick S R Davidson, Petar Vidjen, Sara Trincao-Batra, and Charles A Collin. Older adults' lure discrimination difficulties on the mnemonic similarity task are significantly correlated with their visual perception. 74(8):1298–1307. ISSN 1079-5014, 1758-5368. doi: 10.1093/geronb/gby130.
44. Lubdha M. Shah, Justin A. Cramer, Michael A. Ferguson, Rasmus M. Birn, and Jeffrey S. Anderson. Reliability and reproducibility of individual differences in functional connectivity acquired during task and resting state. 6(5). ISSN 2162-3279, 2162-3279. doi: 10.1002/brb3.456.
45. Leslie A. Zebrowitz, Noreen Ward, Jasmine Boshyan, Angela Gutchess, and Nouchine Hadjikhani. Older adults' neural activation in the reward circuit is sensitive to face trustworthiness. 18(1):21–34. ISSN 1530-7026, 1531-135X. doi: 10.3758/s13415-017-0549-1.
46. Susan Whitfield-Gabrieli and Alfonso Nieto-Castanon. *Conn* : A functional connectivity toolbox for correlated and anticorrelated brain networks. 2(3):125–141. ISSN 2158-0014, 2158-0022. doi: 10.1089/brain.2012.0073.
47. Colleen Hughes, Brittany S. Cassidy, Joshua Faskowitz, Andrea Avena-Koenigsberger, Olaf Sporns, and Anne C. Krendl. Age differences in specific neural connections within the default mode network underlie theory of mind. 191:269–277. ISSN 10538119. doi: 10.1016/j.neuroimage.2019.02.024.
48. Xiaoqian J. Chai, Alfonso Nieto Castañón, Dost Öngür, and Susan Whitfield-Gabrieli. Anticorrelations in resting state networks without global signal regression. 59(2):1420–1428. ISSN 10538119. doi: 10.1016/j.neuroimage.2011.08.048.
49. Jonathan D. Power, Anish Mitra, Timothy O. Laumann, Abraham Z. Snyder, Bradley L. Schlaggar, and Steven E. Petersen. Methods to detect, characterize, and remove motion artifact in resting state fMRI. 84:320–341. ISSN 10538119. doi: 10.1016/j.neuroimage.2013.08.048.
50. Koene R. A. Van Dijk, Trey Hedden, Archana Venkataraman, Karleyton C. Evans, Sara W. Lazar, and Randy L. Buckner. Intrinsic functional connectivity as a tool for human connectomics: Theory, properties, and optimization. 103 (1):297–321. ISSN 0022-3077, 1522-1598. doi: 10.1152/jn.00783.2009.
51. Alexander Schaefer, Ru Kong, Evan M Gordon, Timothy O Laumann, Xi-Nian Zuo, Avram J Holmes, Simon B Eickhoff, and B T Thomas Yeo. Local-global parcellation of the human cerebral cortex from intrinsic functional connectivity MRI. 28(9):3095–3114. ISSN 1047-3211, 1460-2199. doi: 10.1093/cercor/bhx179.
52. Ye Tian, Daniel S. Margulies, Michael Breakspear, and Andrew Zalesky. Topographic organization of the human subcortex unveiled with functional connectivity gradients. 23(11):1421–1432. ISSN 1097-6256, 1546-1726. doi: 10.1038/s41593-020-00711-6.
53. R Core Team. R: A language and environment for statistical computing.
54. John Fox and Sanford Weisberg. *An R companion to applied regression*. SAGE, 2 edition. ISBN 1-5443-3648-9.
55. R Lenth. emmeans: Estimated marginal means, aka least-squares means.
56. C. K. Toner, E. Pirogovsky, C. B. Kirwan, and P. E. Gilbert. Visual object pattern separation deficits in nondemented older adults. 16(5):338–342. ISSN 1072-0502. doi: 10.1101/lm.1315109.
57. Alexander P Christensen. NetworkToolbox: Methods and measures for brain, cognitive, and psychometric network analysis in r. 10(2):422–439. doi: 10.32614/RJ-2018-065.
58. Emily S Finn, Xilin Shen, Dustin Scheinost, Monica D Rosenberg, Jessica Huang, Marvin M Chun, Xenophon Papademetris, and R Todd Constable. Functional connectome fingerprinting: identifying individuals using patterns of brain

connectivity. 18(11):1664–1671. ISSN 1097-6256, 1546-1726. doi: 10.1038/nn.4135.
59. Kwangsun Yoo, Monica D Rosenberg, Wei-Ting Hsu, Sheng Zhang, Chiang-Shan R Li, Dustin Scheinost, R Todd Constable, and Marvin M Chun. Connectome-based predictive modeling of attention: Comparing different functional connectivity features and prediction methods across datasets. 167:11–22. ISSN 1053-8119. doi: 10.1016/j.neuroimage.2017.11.010. Publisher: Elsevier.
60. Gorana Pobric, Elizabeth Jefferies, and Matthew A. Lambon Ralph. Anterior temporal lobes mediate semantic representation: Mimicking semantic dementia by using rTMS in normal participants. 104(50):20137–20141. ISSN 0027-8424, 1091-6490. doi: 10.1073/pnas.0707383104. Publisher: National Academy of Sciences Section: Biological Sciences.
61. Fiona Kumfor, Rosalind Hutchings, Muireann Irish, John R. Hodges, Gillian Rhodes, Romina Palermo, and Olivier Piguet. Do i know you? examining face and object memory in frontotemporal dementia. 71:101–111. ISSN 0028-3932. doi: 10.1016/j.neuropsychologia.2015.03.020.
62. C. J. Mummery, K. Patterson, C. J. Price, J. Ashburner, R. S. J. Frackowiak, and J. R. Hodges. A voxel-based morphometry study of semantic dementia: Relationship between temporal lobe atrophy and semantic memory. 47(1):36–45. ISSN 1531-8249. doi: https://doi.org/10.1002/1531-8249(200001)47:1<36::AID-ANA8>3.0.CO;2-L. _eprint: https://onlinelibrary.wiley.com/doi/pdf/10.1002/1531-8249%28200001%2947%3A1%3C36%3A%3AAID-ANA8%3E3.0.CO%3B2-L.
63. Charan Ranganath and Maureen Ritchey. Two cortical systems for memory-guided behaviour. 13(10):713–726. ISSN 1471-0048. doi: 10.1038/nrn3338. Number: 10 Publisher: Nature Publishing Group.
64. Maureen Ritchey, Laura A. Libby, and Charan Ranganath. Cortico-hippocampal systems involved in memory and cognition: The PMAT framework. In Shane O'Mara and Marian Tsanov, editors, *Progress in Brain Research*, volume 219 of *The Connected Hippocampus*, pages 45–64. Elsevier. doi: 10.1016/bs.pbr.2015.04.001.
65. John P. Aggleton and Malcolm W. Brown. Interleaving brain systems for episodic and recognition memory. 10(10):455–463. ISSN 1364-6613. doi: 10.1016/j.tics.2006.08.003.
66. Wenfeng Zhu, Qunlin Chen, Lingxiang Xia, Roger E. Beaty, Wenjing Yang, Fang Tian, Jiangzhou Sun, Guikang Cao, Qinglin Zhang, Xu Chen, and Jiang Qiu. Common and distinct brain networks underlying verbal and visual creativity. 38(4):2094–2111. ISSN 1097-0193. doi: https://doi.org/10.1002/hbm.23507. _eprint: https://onlinelibrary.wiley.com/doi/pdf/10.1002/hbm.23507.
67. Qi Lin, Monica D Rosenberg, Kwangsun Yoo, Tiffany W Hsu, Thomas P O'Connell, and Marvin M Chun. Resting-state functional connectivity predicts cognitive impairment related to alzheimer's disease. 10:94. ISSN 1663-4365. doi: 10.3389/fnagi.2018.00094. Publisher: Frontiers.
68. Leslie S Gaynor, Rosie E Curiel Cid, Ailyn Penate, Monica Rosselli, Sara N Burke, Meredith Wicklund, David A Loewenstein, and Russell M Bauer. Visual object discrimination impairment as an early predictor of mild cognitive impairment and alzheimer's disease. 25(7):688–698.
69. Christina E. Webb, Chris M. Foster, Marci M. Horn, Kristen M. Kennedy, and Karen M. Rodrigue. Beta-amyloid burden predicts poorer mnemonic discrimination in cognitively normal older adults. 221:117199. ISSN 10538119. doi: 10.1016/j.neuroimage.2020.117199.
70. Richard F. Betzel, Lisa Byrge, Ye He, Joaquín Goñi, Xi-Nian Zuo, and Olaf Sporns. Changes in structural and functional connectivity among resting-state networks across the human lifespan. 102:345–357. ISSN 1053-8119. doi: 10.1016/j.neuroimage.2014.07.067.
71. Bharat B. Biswal, Maarten Mennes, Xi-Nian Zuo, Suril Gohel, Clare Kelly, Steve M. Smith, Christian F. Beckmann, Jonathan S. Adelstein, Randy L. Buckner, Stan Colcombe, Anne-Marie Dogonowski, Monique Ernst, Damien Fair, Michelle Hampson, Matthew J. Hoptman, James S. Hyde, Vesa J. Kiviniemi, Rolf Kötter, Shi-Jiang Li, Ching-Po Lin, Mark J. Lowe, Clare Mackay, David J. Madden, Kristoffer H. Madsen, Daniel S. Margulies, Helen S. Mayberg, Katie McMahon, Christopher S. Monk, Stewart H. Mostofsky, Bonnie J. Nagel, James J. Pekar, Scott J. Peltier, Steven E. Petersen, Valentin Riedl, Serge A. R. B. Rombouts, Bart Rypma, Bradley L. Schlaggar, Sein Schmidt, Rachael D. Seidler, Greg J. Siegle, Christian Sorg, Gao-Jun Teng, Juha Veijola, Arno Villringer, Martin Walter, Lihong Wang, Xu-Chu Weng, Susan Whitfield-Gabrieli, Peter Williamson, Christian Windischberger, Yu-Feng Zang, Hong-Ying Zhang, F. Xavier Castellanos, and Michael P. Milham. Toward discovery science of human brain function. 107(10):4734–4739. ISSN 0027-8424, 1091-6490. doi: 10.1073/pnas.0911855107. Publisher: National Academy of Sciences Section: Biological Sciences.